THERMAL-MECHANICAL ANALYSIS OF ANNULAR FUEL IN COMPARISON TO SOLID FUEL FOR CANDU REACTORS

R. Xu[1]
[1] Atomic Energy of Canada Limited, Chalk River, Ontario, Canada

Abstract

This paper presents an analysis performed using ANSYS finite-element model to simulate the thermal and mechanical responses of annular fuel in comparison to solid fuel under equivalent power ramps at the same coolant conditions. Thermal simulations provided the fuel and sheath temperatures for both fuel designs under an equivalent power ramp while the mechanical simulations predicted fuel and sheath deformation. The results quantify the differences in thermal and mechanical responses between annular fuel and solid fuel designs.

1. Introduction

Internally Cooled Annular Fuel (ICAF) is under consideration for a new high burn-up bundle design at Atomic Energy of Canada Limited (AECL). This new fuel design allows for a potential increase to core power density, while maintaining or improving safety margins. Compared to the traditional solid fuel pin, ICAF increases the heat transfer area and shortens the heat conduction thickness, which is expected to reduce the fuel and sheath temperatures given the same linear power. Consequently, sheath strain is expected to be low since the sheath strain is related to the fuel and sheath temperature.

The objectives of this analysis are to investigate thermal and mechanical responses of annular fuel in comparison to solid fuel under equivalent power ramps at the same coolant conditions, and to quantify the differences in thermal and mechanical responses between these two fuel designs, using the ANSYS finite element code, Version 11.0 [1]. The equivalent power ramp for the annular fuel in comparison to the solid fuel refers to the linear element rating required to achieve an equivalent total bundle power for two different bundle designs. One bundle design comprises only solid fuel elements and the other has annular fuel elements. Since the two bundle designs have a different number of fuel elements, the fuel linear element rating for a single element has to be different for the total bundle power to be the same. For these comparative calculations, the coolant conditions are assumed to be similar to normal operating conditions in current CANDU (CANada Deuterium Uranium) reactors.

The high burn-up bundle is being designed for use in current and future CANDU's. The high burn-up bundle is being designed to fit the current fuelling machines and fuel channels. The ICAF is under consideration for use in high burn-up bundle design. The analysis on ICAF reported in this paper provides technical data to support the high burn-up bundle design, in which the ICAF could be used.

2. Thermal-Mechanical Model

An ANSYS thermal-mechanical coupled model was used to simulate thermal and mechanical responses of an annular fuel element of ICAF design, and a solid fuel element of standard 37-element

fuel bundle design. The ICAF bundle is roughly based on the 28 element bundle used in the Pickering reactors. The element outer diameter is the same as the 28 element bundle (15.2 mm) and the pitch-circle diameter of the outer-two rings of elements are also the same. The centre-four elements are replaced by the single, non-fuelled displacer element. At this stage, it is only a preliminary design and the analysis reported here is for a single fuel element only. This finite element model also provides a base model to be used for more complex boundary conditions.

Both annular fuel and solid fuel were modeled using a one-quarter segment with symmetric boundary conditions in a two-dimensional domain, as the geometric symmetry condition was used to simplify the solution domain. Both heat transfer and deformations in the axial direction were assumed negligible, i.e. results of the simulation represent the solution at a cross-section through the middle of the fuel bundle.

The model geometries and dimensions used in the analysis for the annular fuel design and solid fuel design are shown in Figure 1 and summarized in Table 1, respectively. For the annular fuel design, there was a gap modelled between the fuel and the internal cladding tube, as it was assumed that the internal cladding is not collapsible because the internal cladding would have to balloon to contact the fuel and the coolant pressure is not enough to cause this ballooning. It should be noted that this is a conservative assumption as the predicted fuel temperatures may be a little higher than using a collapsible internal clad. For both designs, there was no gap between the external cladding tube and the fuel as it was assumed a collapsible external clad would be used. In the above assumptions on whether internal and external claddings are collapsible, thermal expansion also plays a role since the fuel has a higher thermal expansion coefficient than the cladding. Figure 2 and Figure 3 shows the 2-D finite element mesh construction in both models, respectively.

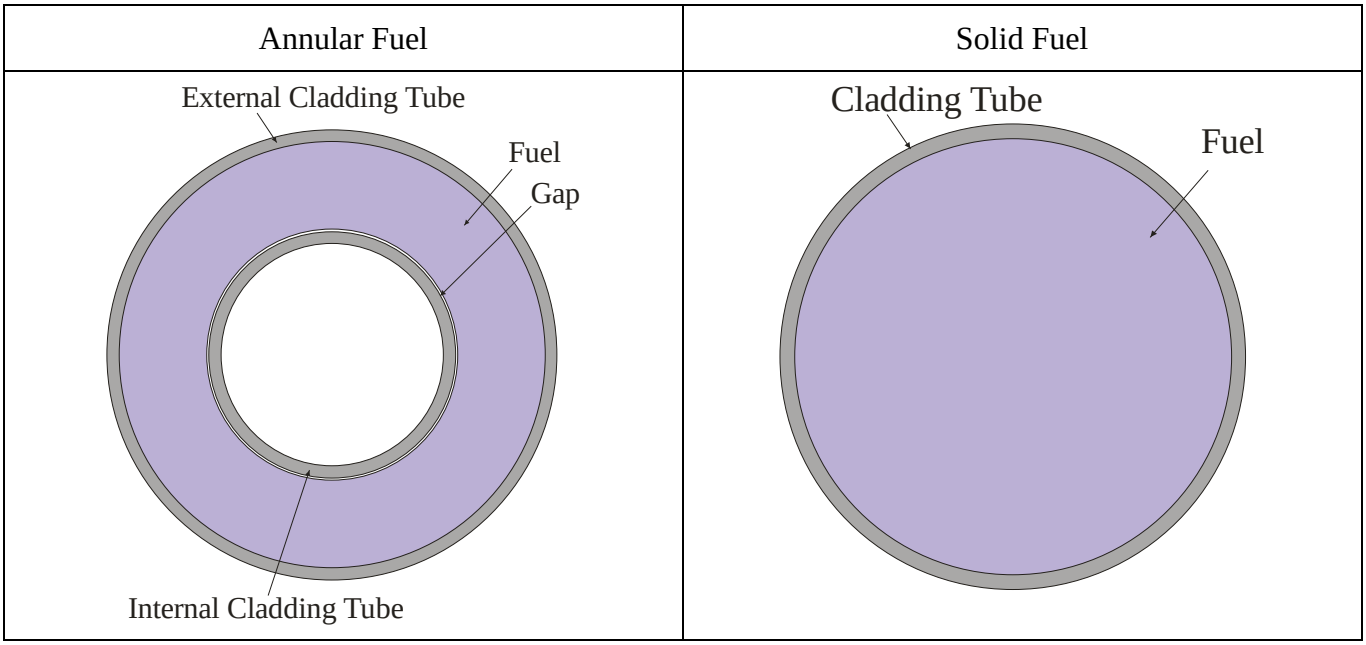

Figure 1 Geometries of Annular Fuel and Solid Fuel.

Table 1 Dimensions of Fuel

	Unit	Solid Fuel	Annular Fuel
Internal Tube ID	mm		7.5
Internal Tube OD			8.32
Fuel ID			8.46
Fuel OD		12.3	14.38
External Tube ID		12.3	14.38
External Tube OD		13.1	15.2

Both solid fuel bundle and ICAF bundle use UO_2 as fuel meat and the temperature-dependent material properties used for UO_2 were those found in Ref. [2]-[4], including density, specific heat, Young's Modulus, Poisson's ratio, thermal conductivity, and thermal expansion coefficient. For the sheath, the material properties of Zircaloy were taken from MATPRO 9 [2]. The material properties are specified at given temperatures in tabular form, and properties between two temperatures are linearly interpolated by the code.

In the thermal model, heat generation was specified as thermal load input on the fuel as a boundary condition. Heat was transferred from the surface of fuel by conduction through the gap to the internal tube and directly to the external cladding tubes. The gap between fuel and internal cladding tube was filled with helium at pressure of 1.5 MPa with a temperature-dependent heat transfer coefficient. A perfect contact was assumed between the surfaces of fuel and external cladding tube. It should be noted that this is a non-conservative assumption as the actual fuel temperatures may be a little higher than predicted, meanwhile it is a reasonable assumption as this paper is about comparing the difference between the fuel types rather than determining absolute temperature. In the fuel and in both tubes, heat was transferred by conduction. Heat transfer was dominated by convective heat transfer from the tube surfaces to the surroundings. The same flow condition was assumed for external flow of both fuel types and also for internal flow of the ICAF. The convective heat transfer coefficient was estimated by using empirical correlations [5] and a value of 29.8 kW/(m^2K) was used.. The bulk fluid temperature of 310°C was assumed to be constant throughout the simulation and variation of the bulk temperature is not considered in this paper. Also, the initial uniform temperature of 310°C was specified for the model.

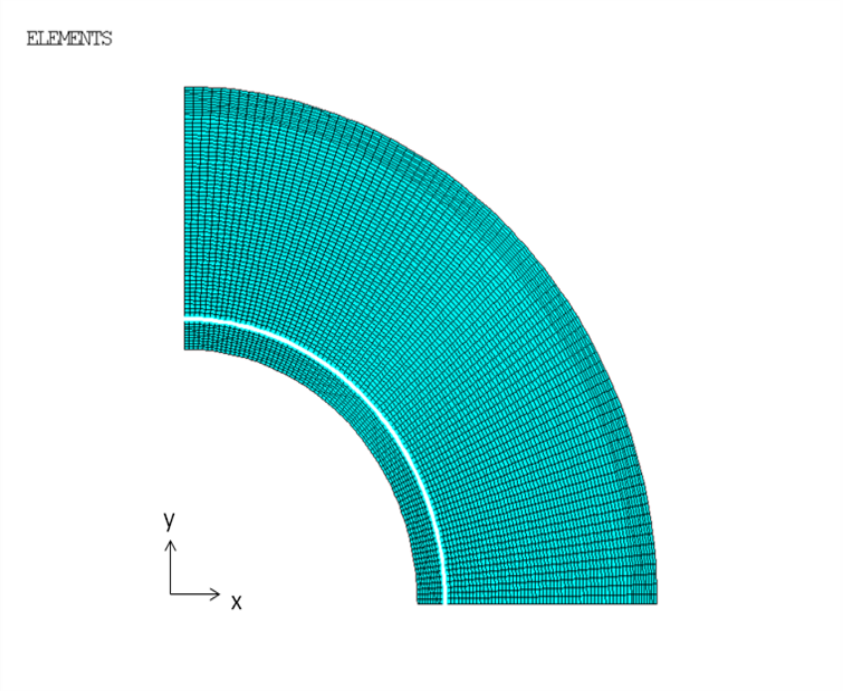

Figure 2 Finite Element Mesh of Annular Fuel.

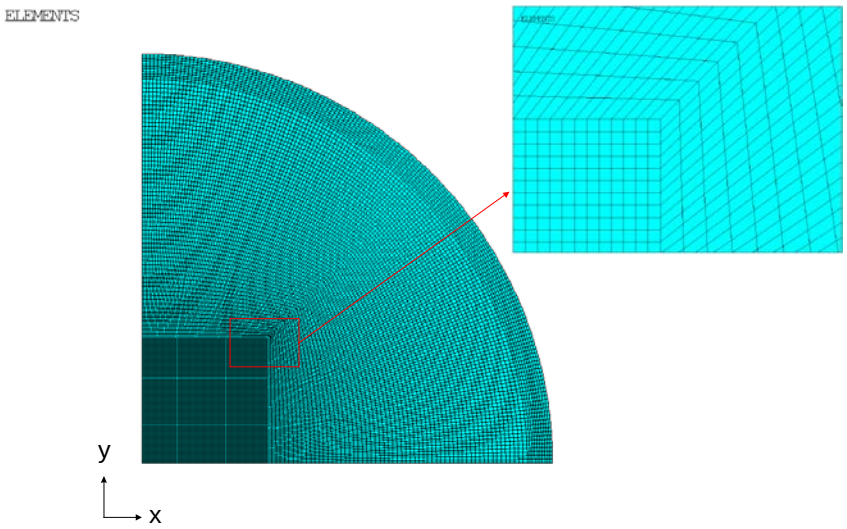

Figure 3 Finite Element Mesh of Solid Fuel.

The same mesh was used in the thermal model and mechanical model. The ANSYS element types PLANE55 and PLANE182 were used in the thermal model and mechanical model, respectively. Thermal-mechanical coupling occurs by applying load terms from thermal analysis to stress analysis across a node-to-node similar mesh interface. The temperature distribution on the fuel and cladding tubes from the thermal model was read from the thermal results file and applied as loads in the

mechanical model. Pressure of 10 MPa was applied to the surfaces of both internal (for annular fuel only) and external cladding tubes. Pressure of 1.5 MPa was applied to the surfaces of fuel and internal cladding tube in the gap for annular fuel. Then, simulation post processing was performed and simulation results, including temperature, displacement, stress and strain, were extracted from data files.

3. Results

3.1 Thermal-Mechanical Responses of Annular Fuel

The ANSYS thermal-mechanical simulations predicted temperature distribution, displacement, stress and strain for three power ramps, with initial powers of 25.7, 46.2, 65.45 kW/m and final powers of 102.6, 92.4, 84.7 kW/m, respectively, for a single fuel pin. The term “power ramp” here refers to linear power increases from one steady state (initial power) to another steady state (final power). Therefore, static analysis was performed for each power state.

Figure 4 to Figure 6 show results of the simulations for annular type fuel for the case of 25.7 to 102.6 kW/m at final power, including displacement, temperature, and strain. Table 2 summarizes the simulation results for annular fuel. In all three cases, heat was transferred radially from the fuel and temperature decreased from the middle of the fuel in both inward and outward radial direction to the surfaces of both cladding tubes. Displacement in the radial direction increased along the radial direction and the maximum occurred at the outside surface of the external cladding tube. Strain varied along the radial direction and reached a maximum value at the outside surface of the external cladding tube. The maximum strain and displacement occur near the outside surface in the area of maximum stress, rather than near the maximum temperature. The maximum temperature occurs toward the inner half of the annular fuel, as the heat transfer path to the coolant through the gas gap and the cladding tube on the internal surface has a higher resistance to heat flow than the perfect contact (no gap) assumed at the outside surface. As a result of the power ramp from 25.7 kW/m to 102.6 kW/m, the maximum temperature in the fuel increased from 418°C to 783°C; the maximum displacement was about 0.0467 mm; and the maximum strain increased from an initial state of 0.17% to final state of 0.39%. As a result of the power ramp from 46.2 kW/m to 92.4 kW/m, the maximum temperature in the fuel increased from 508°C to 730°C; the maximum displacement was about 0.0441 mm; and the maximum strain increased from initial state of 0.23% to final state of 0.36%. As a result of the power ramp from 65.45 kW/m to 84.7 kW/m, the maximum temperature in the fuel increased from 598°C to 692°C; the maximum displacement was about 0.0421 mm; and the maximum strain increased from initial state of 0.28% to final state of 0.34%.

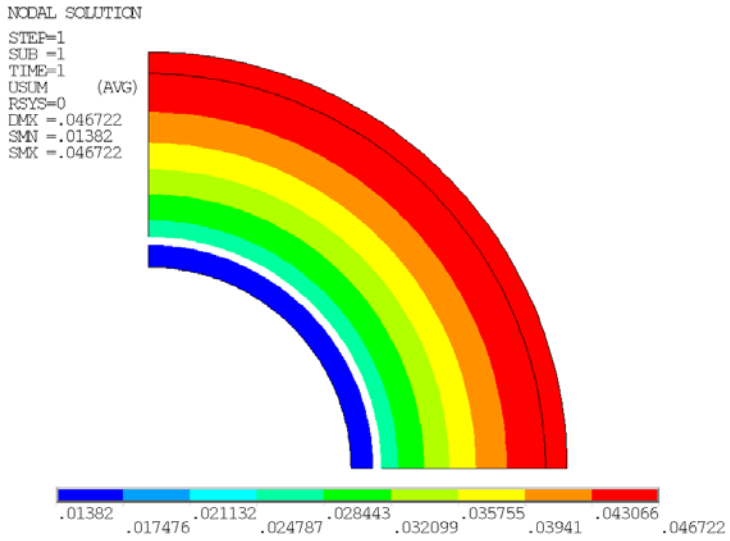

Figure 4 Simulated Displacement (mm) in Thermal-Mechanical Responses of Annular Fuel.

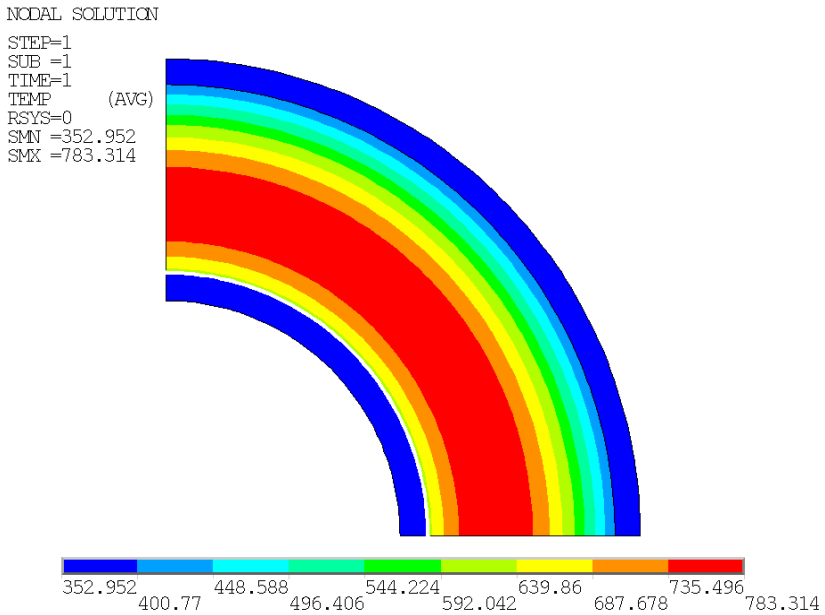

Figure 5 Simulated Temperature (°C) in Thermal-Mechanical Responses of Annular Fuel.

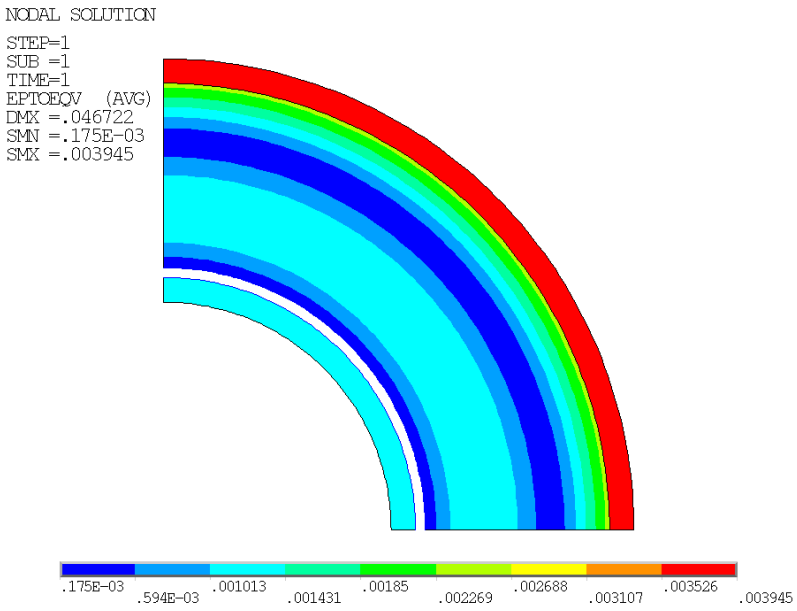

Figure 6 Simulated Strain in Thermal-Mechanical Responses of Annular Fuel.

Table 2 Summary of Simulation Results for Annular Fuel

Design	Power Ramp Scenario	Result	Unit	Initial Power	Final Power	Difference
CANDU Design Annular Fuel	Case 1	Displacement	mm	0.028	0.0468	0.0188
		Temperature	°C	418	783	365
		Strain	%	0.17	0.39	0.22
	Case 2	Displacement	mm	0.0328	0.0441	0.0113
		Temperature	°C	508	730	222
		Strain	%	0.23	0.36	0.13
	Case 3	Displacement	mm	0.0374	0.0421	0.0047
		Temperature	°C	598	692	94
		Strain	%	0.28	0.34	0.06

3.2 Thermal-Mechanical Responses of Solid Fuel

As a comparison with annular fuel, thermal-mechanical responses of solid fuel were simulated. Three cases of power ramp, which are equivalent in terms of total bundle power to the three power ramp cases for annular fuel, were simulated using the ANSYS model.

The ANSYS thermal-mechanical simulations predicted temperature distribution, displacement, stress and strain for three power ramps, with initial power of 20.3, 36.6, 51.85 kW/m and final power of 81.3, 73.2, 67.1 kW/m, respectively.

Figure 7 to Figure 9 show results of the simulations for solid fuel for the case of 20.3 to 81.3 kW/m at final power, including displacement, temperature, and strain. Table 3 summarizes the simulation results for solid fuel. The center of the fuel rod was always the hottest location and temperature decreased in the radial direction from the center to the outside surface of the cladding tube. Displacement increased in the radial direction. Strain varied in the radial direction and reached a maximum value at the outside surface of the cladding tube. The maximum strain and displacement occurred near the outside surface in the area of maximum stress, rather than near the maximum temperature. As a result of the power ramp from 20.3 kW/m to 81.3 kW/m, the temperature at the center of the fuel rod increased from 691°C to 2807°C; the maximum displacement was about 0.0897 mm; and the strain increased from initial state of 0.29% to final state of 1.21%. As a result of the power ramp from 36.6 kW/m to 73.2 kW/m, the temperature at the center of the fuel rod increased from 1094°C to 2516°C; the maximum displacement was about 0.0807 mm; and the strain increased from initial state of 0.47% to final state of 1.06%. As a result of the power ramp from 51.85 kW/m to 67.1 kW/m, the temperature at the center of the fuel rod increased from 1691°C to 2296°C; the maximum displacement was about 0.074 mm; and the strain increased by about 0.26% from initial state of 0.7% to final state of 0.96%.

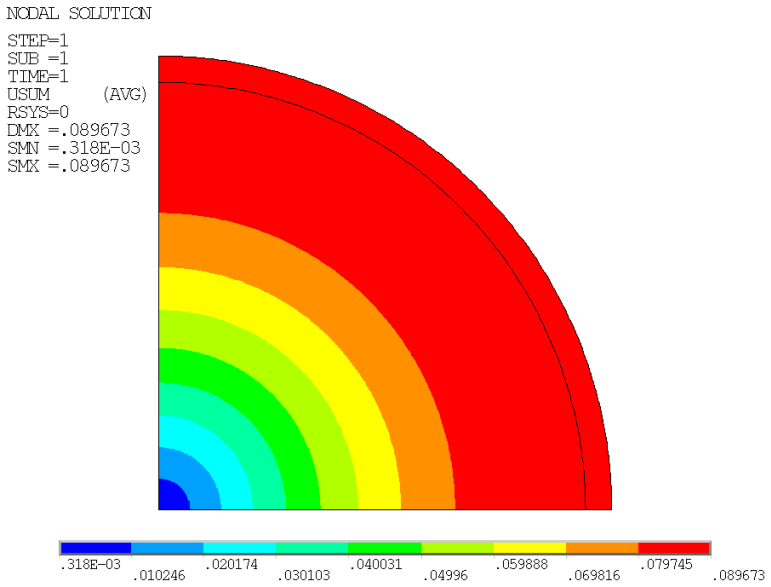

Figure 7 Simulated Displacement (mm) in Thermal-Mechanical Responses of Solid Fuel.

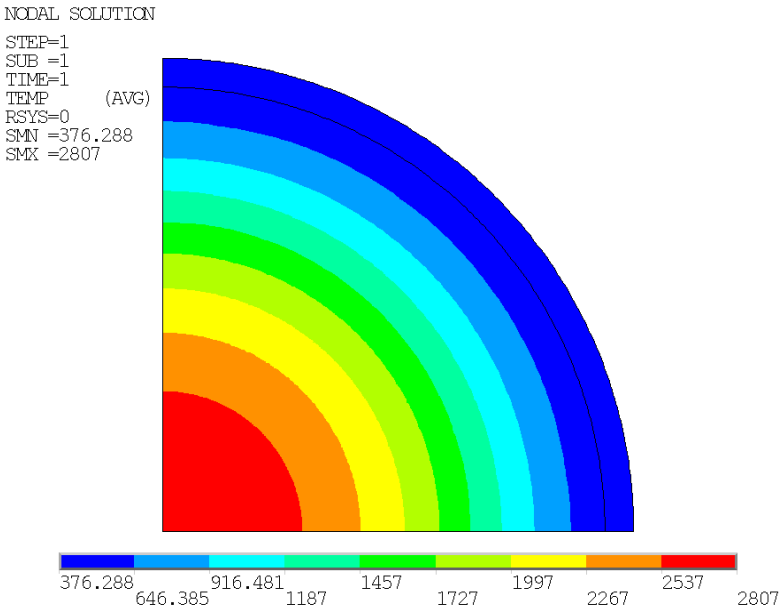

Figure 8 Simulated Temperature (°C) in Thermal-Mechanical Responses of Solid Fuel.

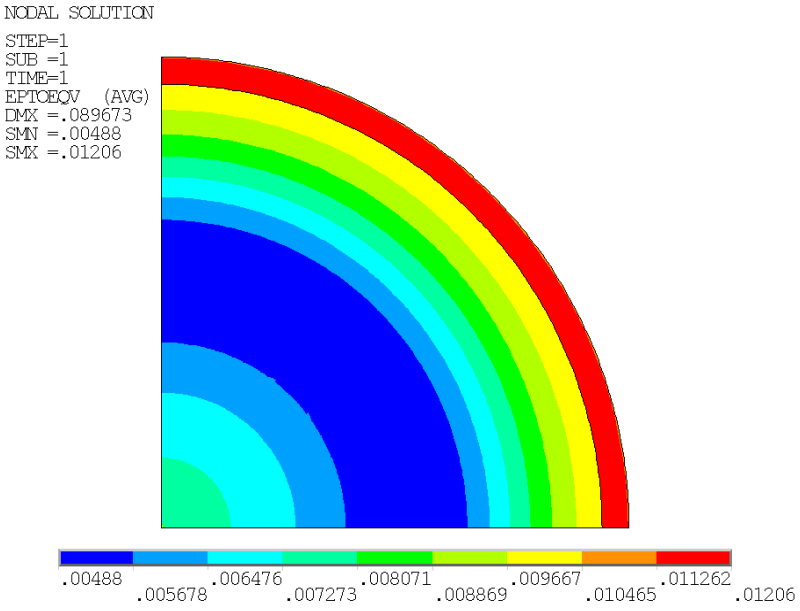

Figure 9 Simulated Strain in Thermal-Mechanical Responses of Solid Fuel.

Table 3 Summary of Simulation Results for Solid Fuel

Design	Power Ramp Scenario	Result	Unit	Initial Power	Final Power	Difference
CANDU Design Solid Fuel	Case 1	Displacement	mm	0.0313	0.0897	0.0584
		Temperature	°C	691	2807	2116
		Strain	%	0.29	1.21	0.92
	Case 2	Displacement	mm	0.0428	0.0807	0.0379
		Temperature	°C	1094	2516	1422
		Strain	%	0.47	1.06	0.59
	Case 3	Displacement	mm	0.0574	0.074	0.0166
		Temperature	°C	1691	2296	605
		Strain	%	0.7	0.96	0.26

4. Discussion

A thermal-mechanical analysis was performed for a single annular fuel of CANDU bundle design in comparison to solid fuel element design of standard 37-element fuel bundle by using a two-dimensional ANSYS model. Temperature distributions, displacement, stress and strain were predicted for different power ramp cases.

For the bundle design with annular fuel, the maximum temperature ranged from 418°C to 783°C and the maximum strain ranged from 0.17% to 0.39%, for a linear element ratings ranging from 25.7 to 102.6 kW/m. Correspondingly, for the solid element design comprising solid fuel, the maximum fuel temperature ranged from 691 to 2807°C and the maximum strain ranged from 0.29% to 1.21%, for similar bundle powers and lower linear element ratings (20.3 to 81.3 kW/m).

The comparison of analysis results of these two different fuel designs clearly reveals that both the maximum temperature and strain of annular fuel are much lower than that of solid fuel, which is operating at a lower linear power rating to achieve the equivalent bundle power. Also, the temperature and strain increases in annular fuel as a result of increasing the linear element rating are much lower than that of the solid fuel experiencing an equivalent power increase. The above results can be attributed to an extra cooling effect provided by the constant-temperature coolant flow through the interior of the annular fuel pin, as it is the main difference between annular fuel and solid fuel designs. With the extra cooling effect in the annular fuel, the annular fuel produces lower thermal-mechanical responses than solid fuel at equivalent linear power rating, which provides larger margin for the annular fuel to be operated at higher linear element rating.

5. Conclusion

It can be concluded that the annular fuel would be able to operate at a higher linear element rating than the solid fuels with lower sheath strains due to the improved cooling provided by the coolant flow through the interior of the annular fuel. The analysis can be further improved by incorporating more realistic coolant conditions and experimentally measured gap conductances between the fuel and the internal cladding tube and the external cladding tube in the solid and annular fuel models. The conclusion is based on the analysis performed under specified conditions and more analysis with further improved model is needed to confirm this conclusion.

6. References

[1] ANSYS Inc., "ANSYS Theory Reference 11.0", Canonsburg, PA, 2007

[2] "MATPRO – Version 09, A Handbook of Materials Properties for Use in the Analysis of Light Water Reactor Fuel Rod Behaviour", TREE-NUREG-1005, 1976

[3] P.G. Lucuta, H. Matzke and I.J. Hastings, "A Pragmatic Approach to Modelling Thermal Conductivity of Irradiated UO_2 Fuel: Review and Recommendations", J. Nucl. Mater., 166-232, 1996

[4] "MATPRO – Version 11, A Handbook of Materials Properties for Use in the Analysis of Light Water Reactor Fuel Rod Behaviour", NUREG/CR-0497, TREE-1280, Rev. 2, 1981

[5] Y.A. Cengel, "Heat Transfer: A Practical Approach", 2nd Edition, McGraw, 2003